

# Analytical Model for Gravity and Rayleigh-Wave Investigation in the Layered Ocean–Earth Structure

by Tatyana Novikova, Kuo-Liang Wen, and Bor-Shouh Huang

**Abstract** In terms of the linear theory of elasticity we analyze the gravity and Rayleigh-wave excitation and propagation process in a three-layered ocean–Earth model, which includes a superficial liquid layer and two layers of sediments—soft and hard. To compute the oceanic surface-wave dispersion function, the Thomson-Haskell matrix method is used. The solution is obtained by applying the normal mode formalism to the flat, homogeneous, layered ocean–Earth structure. Based on this theory, the spectra of the excitation functions are investigated in detail for 45° thrust, dip-slip, and strike-slip point sources in the half-space.

A numerical experiment reveals that the rigidity of the rock exerts a strong influence on both gravity and Rayleigh waves. In the case of Rayleigh waves, a layered structure of the bottom strongly affects the propagation process.

The main focus of the present study is to model tsunami and tsunamigenic events. It is well known from observations that earthquakes that generate abnormally large tsunamis are mostly thrust events, characterized by long source duration (2–4 times longer than typical earthquakes of similar moment) and shallow source depth, and are located near the trench axis. Meanwhile, typical tsunamigenic earthquakes are generally dip-slip and thrust events with depths between 15 and 50 km. On this basis, and using the distributed model of seismic source, the influence of source mechanism, location, and source duration on the tsunami-wave amplitude are investigated here.

The results of our model computations of the seismic sea waves from tsunami- and tsunamigenic earthquake are in good agreement with real observation data.

## Introduction

### Study of Tsunami and Oceanic Rayleigh Waves in the Coupled Ocean–Earth Model

The problem with regard to tsunami and Rayleigh-wave excitation and propagation has long been the subject of investigations. Efforts have been made to study issues both analytically, as in the case of uniform depth (Pod'yapol'sky, 1970; Alexeev and Gusiakov, 1974; Yamashita and Sato, 1974; Ward, 1980; Comer, 1984a,b; Okal, 1988), and numerically, as with actual bathymetry (e.g., Hwang, 1972; Satake, 1985, 1995; Mayers and Baptista, 1995; Imamura, 1995).

At present, with respect to the study of tsunami generation, propagation, and run-up, numerical modeling techniques are extremely important. They can be successfully applied to find solutions to different aspects of tsunami-related problems, such as in the study of the source process, the synthesis of tsunami run-up heights in an offshore zone, and the impact on coastal structures. Various techniques, usually designed for computations as tsunami generation and run-up, were critically summarized by Shuto (1991). He re-

viewed the fundamental equations and difference schemes for the solution to the nonlinear problem of tsunami-wave propagation in the near-shore zone. According to his analysis, numerical simulations provide only approximate solutions with more or less satisfactory information for practical use but inevitably embedded with errors depending on the numerical techniques. He estimated that the maximum of tsunami run-up heights based on numerical computations had an error of margin of less than 15%. However, in some cases, such as the 1992 Nicaragua earthquake, heights of the tsunami run-up are much larger than those obtained numerically. Therefore, it is necessary to undertake analytical investigations.

Analytical description of ocean surface-wave generation and propagation is usually based on the fully or partially coupled ocean–Earth models. Comer (1984b), using a solution for the tsunami mode excitation due to a point moment tensor earthquake source in the flat Earth, has demonstrated that both approaches yield nearly identical results.

In the present study we use the first approach, which

involves the normal mode technique. We therefore review briefly the previous works in this direction.

Originally the idea of using the fully coupled ocean–solid Earth model for the analysis of tsunami generation was proposed by Pod'yapol'sky (1968, 1970). He rigorously investigated the mathematical statement of the problem and showed that it is equivalent to the usual system of motion equations of the dynamic elasticity theory in the limit of negligible gravity and to the linear theory of long waves in the limit of incompressible liquid and rigid bottom. For the point source, he obtained the general solution, proved the existence of a gravitational root of the dispersion equation, and in an approximation of uncompressible liquid, derived asymptotic formulae for the amplitude of gravity waves in liquid at large epicentral distances. Studying the dependence of tsunami generation on the seismic source parameters, Pod'yapol'sky pointed out that there exists some optimal source depth. He also obtained estimates of the fraction of the seismic energy spent to generate a tsunami.

Later Yamashita and Sato (1974, 1976) applied the same coupled model to Rayleigh-wave generation and shed some new light on tsunami excitation studies. In particular, by modeling an earthquake with a dip-slip point dislocation and with a finite-moving source, they looked into the influence of focal parameters—dip-angle, fault length, and focal depth—on tsunami and Rayleigh waves. They showed that a dip-angle affects a Rayleigh wave in the opposite way that it does a tsunami: for instance, when the dip angle is large, a small Rayleigh wave but a large tsunami are generated. Other focal parameters seem to have similar effects on Rayleigh and tsunami waves. Yamashita and Sato (1976) emphasized that a model of layered oceanic crust is more appropriate for the study of Rayleigh waves since Rayleigh waves depend considerably on the layered structure.

Investigations of tsunami excitation in the coupled system were continued by Ward (1980, 1981) and Comer (1984a,b). Describing tsunamis as free oscillations of a spherically symmetric self-gravitating Earth (Okal, 1978) and using a moment tensor representation of both point and line seismic sources, Ward derived expressions for tsunami-wave displacement in the near- and far-field zones. He found that tsunami mode excitation was strongly influenced by the moment, mechanism, and depth of the source. To compare the computed tsunami waveforms with observations, Ward (1982a,b) extended the study to a general double-couple source. Analyzing the Kurile Islands event of 13 October 1963 (which belongs to the class of “tsunami-earthquake” events), he found that although the earthquake mechanism does play a critical role in tsunami production, many sources have nearly equal tsunami moment and nearly equal ability for sea-wave excitation.

Similar to Ward, Comer (1984a) assumed the ocean to be nonviscid and only considered the linearized equations of motion and boundary conditions. He emphasized that basically tsunamis are ocean-surface long-period gravity waves and that elastic terms in the ocean are of secondary importance and therefore retained only the most important forces

in the motion equations. The difference from Ward's study (1980) is that Comer (1984a) applied normal mode formalism to the tsunami excitation by a point source in the flat Earth. As he emphasized, the normal modes of a finite body form a complete basis for small amplitude oscillations of the body, but those of an infinite body, like the flat Earth, do not.

Okal (1988) applied the normal mode formalism to the spherically symmetric self-gravitating and elastic ocean–Earth model with a 1-km-thick sedimentary layer in between. Having investigated tsunami (long-period gravity waves) excitation by seismic sources in a sedimentary layer, he showed theoretically that the excitation of a tsunami by a thrust-fault mechanism can gain one order of magnitude by just locating 10% of the moment release inside a layer with weaker mechanical properties. In other words, the sedimentary structures provide amplification for tsunami excitation. Another important conclusion of his study is that the bathymetry variations along the path of tsunami waves can result in focusing and defocusing effects and thus strongly influence the final amplitude in the offshore zone.

It is essential to note that all of the examples described previously dealt with models consisting of a liquid layer half-space. The only exception is Okal's (1988) study, in which he used a model with a sedimentary layer in between to explore some physical aspects of the role of sediments in tsunami excitation.

In the present study, we take the ocean–Earth model consisting of the compressible liquid (ocean), soft (unconsolidated), and hard (consolidated) sediments resting on the elastic half-space. First, this model provides an appropriate description of the Rayleigh waves, which highly depend on the layered structure (Yamashita and Sato, 1976). Second, when applied to gravity waves, a model with low-rigidity layers also makes it possible to study tsunami earthquakes, the mechanism of which has never been clearly understood until now.

A number of hypotheses have been proposed to explain anomalous tsunami excitation by an earthquake with relatively small magnitude. Most common among them are the source rupture times of unusually long duration (Kanamori, 1972), non-double-couple sources such as submarine landslides (Hasegawa and Kanamori, 1987), the underestimation of the actual seismic moment from surface waves due to shallow source depth and fault angle (Ward, 1982a), and shallow faulting within sediments accompanied by a change in fault orientation during the rupture (Fukao, 1979; Okal, 1988).

Pelayo and Wines (1992), based on the study of the long-period surface waves from the 1896 Sanriku earthquake ( $M_w$  7.6) and the 1946 Aleutian earthquake ( $M_w$  7.4), which represent the most abnormal events among this class, suggested that the double-couple (faulting) mechanism for such events is more likely than a single force mechanism that represents landslides. They also concluded that tsunami-earthquakes are mostly thrust-faulting events characterized by long source duration, very shallow fault dip ( $6^\circ$ – $8^\circ$ ), and

shallow source depth (less than 15–20 km), and are most commonly located near deep-sea trenches. The long source duration is a consequence of their occurrence within lower-velocity sedimentary layers. One of the important results of the study is the slow rupture and long source duration result in poor excitation of seismic frequencies used in magnitude determination such that the earthquakes are much larger than indicated by traditional magnitudes.

Kanamori and Kikuchi (1993), using previously accumulated experience in tsunami investigations, distinguished two types of tsunami earthquakes: very anomalous and moderate. A very anomalous tsunami earthquake occurs at an accreting margin with large amounts of sediments and an accretionary prism, where occasional slumping causes the tsunami earthquake (1896 Sanriku, 1946 Aleutian, 1975 Unimak Islands, 1999 Papua New Guinea). A moderate tsunami earthquake occurs in a subduction zone with a thin sedimentary layer, where a slow rupture in the subducted sediments is responsible for a large tsunami (1960 Peru; 1963, 1975 Kurile Islands; 1992 Nicaragua).

Among the large amount of research that focuses on the understanding of tsunami earthquake mechanism, the recent study made by Seno (2000) undoubtedly is one of the most interesting. He analyzed the 1999 Chi-Chi earthquake in Taiwan. This event was associated with abnormally uplifted area in the northwestern corner of the earthquake fault. Such inelastic uplifts would imply an abnormal tsunami if the area were under the sea. Using for analysis the Global Positioning System data and sand box experiment over the ductile décollements, Seno suggested a new factor for the mechanism of tsunami earthquakes: an uplift of the sediment or weak accretionary prism caused by a sudden horizontal movement on the décollement beneath the lowermost inner trench slope like sand being pushed up by a bulldozer.

The purpose of this article is to present an analytical model of tsunami and Rayleigh waves in the layered ocean–Earth structure, and, of particular relevance to tsunami-earthquakes studies, to explore the influence of the different rigidity of the layers on the wave excitation intensity.

### Numerical Techniques for the Surface-Wave Computations in the Multilayered Ocean–Earth Model

In our model the ocean–Earth structure is represented by parallel, horizontal layers with given thickness and mechanical properties. In such a system we solve the one-dimensional boundary problem for the eigenvalues and eigenfunctions corresponding to the surface waves of Rayleigh type. To solve the problem of surface-wave propagation in the stratified media the matrix formulations are usually used (Thomson, 1950; Haskell, 1953; Knopoff, 1964; Gilbert and Backus, 1966).

Originally, Thompson (1950) and Haskell (1953) developed the theoretical background for a study of Rayleigh and Love surface-wave dispersion in the multilayered Earth model, yielding additional information about the structure of

the upper mantle. In their theory, the period equation yields a product of  $4 \times 4$  matrices, one per layer, each being a function only of the period, phase velocity, and the parameters of a single layer. These layer matrices relate the components of motion at one interface in a layered structure to those at the next. Dorman *et al.* (1960) applied Haskell's matrix-iteration theory for the computation of Rayleigh-wave dispersion for 11 models of the continental and oceanic crust-mantle systems to study the shear velocity distribution in the upper mantle. They found an agreement between velocity distributions for the continental crust mantle from body-wave data (obtained by Gutenberg (1926) and by Lehmann (1955)) and from Rayleigh-wave dispersion data.

A source at depth in a multilayered formation was introduced to determine the effect of source location on surface-wave amplitudes. This excitation problem was successfully solved by Haskell (1964), who determined the radiation pattern of surface waves from the following types of seismic sources: a single force, a force dipole without torque, and a single couple. Harkrider (1964) extended such investigations to the case of Rayleigh waves in a multilayered model with a superficial liquid layer. The source theory he developed has become a foundation for the computations of amplitude spectra and synthetic seismograms under various conditions of source type, structure, and source depth. He found that the radiation pattern of Rayleigh waves strongly depends on the depth of the source and, unlike the fundamental Love mode, is sensitive to small variations in frequency.

Modal calculations of the wave propagation in the layered media exhibit numerical difficulties at high frequencies: when the frequencies become large, the matrix components are very large and the periodic function loses significance, making it impossible to obtain accurate values of the roots. Using Haskell layer matrices, Knopoff (1964) proposed an alternate method for constructing the matrix representation of the dispersion function for surface waves, which avoids such difficulties at high frequencies. His formulation is based on the immediate construction of the dispersion function, and then the determinant is decomposed into a product of interface matrices, which is derived from submatrices of the determinant. Each of these interface submatrices relates the components of motion across the interface between two adjacent layers. Employing the Knopoff method, Randall (1967) developed a computer program. Later, Watson (1970) and Schwab (1970) modified matrix formulas for model solutions in the layered, elastic half-space to enable faster machine computation.

In short, both the analytical and the numerical approaches in the study of ocean surface waves play equally important roles and must develop simultaneously to obtain better agreement between theory and observations.

### Statement of the Problem

The model we used to study gravity and Rayleigh-wave propagation consists of three homogeneous, isotropic layers

overlying the homogeneous half-space. A superficial layer of uniform thickness  $H$  was assumed to be a compressible nonviscid liquid. Between the liquid and the half-space, there are two layers of sediments: soft and hard.

In such a system the equations of motion are written in the linear theory approximation (Pod'yapol'sky, 1968, 1970; Gusiakov, 1975):

$$\lambda_0 \nabla \operatorname{div} \mathbf{u} - \rho_0 g \mathbf{e}_z \operatorname{div} \mathbf{u} = \rho_0 \frac{\partial^2 \mathbf{u}}{\partial t^2} \text{ at } 0 < z < H, \text{ and} \quad (1)$$

$$(\lambda_m + 2\mu_m) \nabla \operatorname{div} \mathbf{u} - \mu_m \operatorname{curl}(\operatorname{curl} \mathbf{u}) = \rho_m \frac{\partial^2 \mathbf{u}}{\partial t^2} \text{ at } z > H. \quad (2)$$

Here  $c_f$  is the velocity of the acoustic wave in the liquid layer;  $\lambda_0$ ,  $\lambda_m$ , and  $\mu_m$ , and  $\rho_0$ ,  $\rho_m$  are the Lamé parameters and densities of the liquid and solid medium, respectively;  $\mathbf{u}_i = (U_i, 0, W_i)$  is the displacement vector ( $i = 0$  for liquid layer,  $i = m$  for sedimentary layers, and  $i = n$  for half-space),  $g$  is gravity;  $\omega$  is the angular frequency; and  $z$  is the depth from the free surface (positive downward).

For the oceanic model (Fig. 1) boundary conditions to be satisfied are as follows: the vanishing of pressure at the *surface* of the liquid layer (free surface); the continuity of normal component displacement and stress and the vanishing of shear stress at the liquid-solid interface (zeroth interface); the continuity of two displacement and stress and the components at each solid-solid interface (starting from the first one); and the vanishing of the displacement at  $z \rightarrow \infty$ .

### Solution

We seek the solution of the motion equations in the form of a plane wave propagating in the horizontal direction of increasing  $x$  with frequency  $\omega$  and the amplitude decreasing exponentially in the positive downward  $z$  direction in the half-space:

$$\mathbf{u}_i(x, z, w, t) = \mathbf{v}_i(z, \omega) \exp[i\omega(t - x/c)]. \quad (3)$$

Substituting (3) into equations (1) and (2) and introducing the boundary condition at  $z \rightarrow \infty$ , wave amplitudes as a function of depth yield

$$U_0(z, \omega) = \frac{ic_f^2}{\omega c} [-A_0 \exp(-\eta_{02}z/c_f) + B_0 \exp(-\eta_{01}z/c_f)], \quad (4)$$

and

$$W_0(z, \omega) = -\frac{c_f}{\omega^2} [-\eta_{01}A_0 \exp(-\eta_{02}z/c_f) + \eta_{02}B_0 \exp(-\eta_{01}z/c_f)], \quad (5)$$

for the liquid layer, where

$$\eta_{01} = -\omega\gamma - g/2c_f, \quad (6)$$

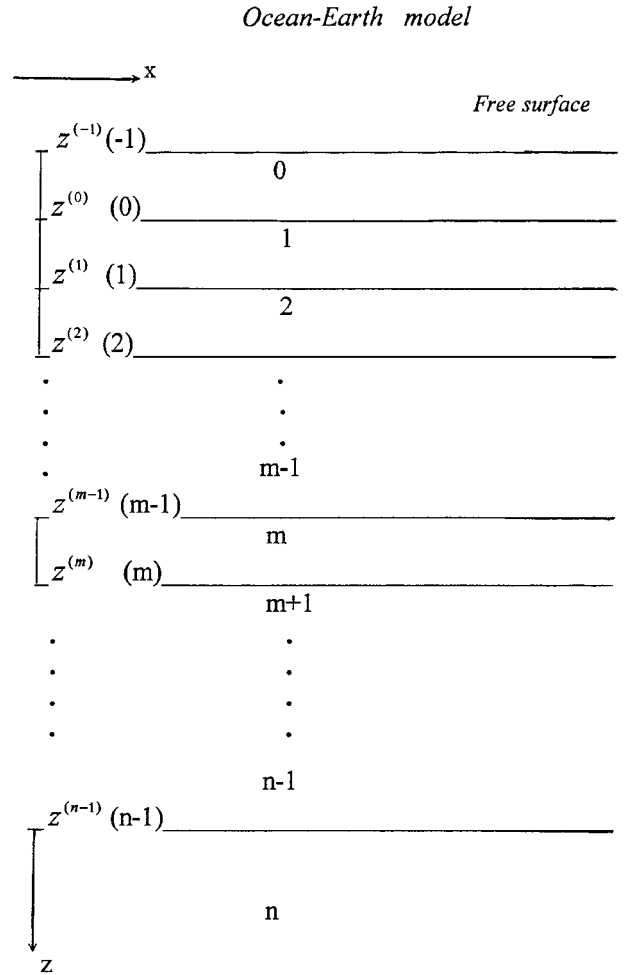


Figure 1. Coordinate system and geometry of the problem.

$$\eta_{02} = \omega\gamma - g/2c_f, \text{ and} \quad (7)$$

$$\gamma^2 = \frac{c_f^2}{c} - 1 + \frac{g^2}{4c_f^2\omega^2}, \quad (8)$$

for the sedimentary layers:

$$U_m(z, \omega) = \frac{ia_m^2}{\omega c} ((C_m \exp(-\omega\alpha_m z/a_m) + D_m \exp(\omega\alpha_m z/a_m)) - \frac{i\beta_m b_m}{\omega} (E_m \exp(-\omega\beta_m z/b_m) + F_m \exp(\omega\beta_m z/b_m))), \quad (9)$$

$$W_m(z, \omega) = \frac{\alpha_m a_m}{\omega} (C_m \exp(-\omega\alpha_m z/a_m) + D_m \exp(\omega\alpha_m z/a_m)) - \frac{\beta_m^2}{\omega c} (E_m \exp(-\omega\beta_m z/b_m) + F_m \exp(\omega\beta_m z/b_m)), \quad (10)$$

and for the half-space,

$$U_n(z, \omega) = \frac{ia_n^2}{\omega c} C_n \exp(-\omega \alpha_n (z-H)/a_n) - \frac{ib_n \beta_n}{\omega} E_n \exp(-\omega \beta_n (z-H)/b_n), \quad (11)$$

and

$$W_n(z, \omega) = \frac{a_n \alpha_n}{\omega} C_n \exp(-\omega \alpha_n (z-H)/a_n) - \frac{b_n^2}{\omega c} E_n \exp(-\omega \beta_n (z-H)/b_n), \quad (12)$$

where

$$\alpha_{m,n}^2 = \begin{cases} i(1 - a_{m,n}^2/c^2)^{1/2} & \text{if } c > a_{m,n} \\ (a_{m,n}^2/c^2 - 1)^{1/2} & \text{if } c < a_{m,n} \end{cases}$$

$$\beta_{m,n}^2 = \begin{cases} i(1 - b_{m,n}^2/c^2)^{1/2} & \text{if } c > b_{m,n} \\ (b_{m,n}^2/c^2 - 1)^{1/2} & \text{if } c < b_{m,n} \end{cases}$$

The system of the boundary conditions represents a number of homogenous equations with unknown coefficients. To determine these later, the periodic equation has to be solved. The Thomson-Haskell technique is used here to construct the dispersion function. The idea of the method is the creation of the layer matrices that relate the components of motion at one interface in a layered structure to those at the next. The product of these layer matrices then relates the components of motion at the deepest interface to those at the free surface, and this layer-matrix product is then used to construct the dispersion function.

Following Haskell (1953), for the convenience in performing the calculation of the periodic function, we write down the boundary conditions in matrix form, starting with the free surface that is free from stress:

$$L_0 \begin{pmatrix} A_0 \\ B_0 \end{pmatrix} = 0, \quad (13)$$

where

$$L_0 = \begin{pmatrix} -c_f^2 - \frac{gc_f \chi_1}{\omega^2}, c_f^2 + \frac{gc_f \chi_2}{\omega^2} \end{pmatrix},$$

$$\chi_1 = -\omega\gamma - \frac{g}{2c_f}, \chi_2 = \omega\gamma - \frac{g}{2c_f}.$$

To satisfy this condition we have to allow that

$$A_0 = N_0 \left( 1 - \frac{g^2}{2c_f^2 \omega^2} + \frac{g\gamma}{c_f \omega} \right), \text{ and } B_0 = N_0 \left( 1 - \frac{g^2}{2c_f^2 \omega^2} - \frac{g\gamma}{c_f \omega} \right),$$

where  $N_0$  is constant.

Dorman (1962) provided an expression to describe the case where the series of the liquid layers are present in the model.

At the liquid-solid interface:

$$\begin{pmatrix} kW \\ p_{zz} \end{pmatrix} = ME_0 \begin{pmatrix} A_0 \\ B_0 \end{pmatrix}, \quad (14a)$$

where

$$M = \begin{pmatrix} \frac{c_f \eta_{01}}{\omega} & -\frac{c_f \eta_{02}}{\omega} \\ \rho_f (-c_f^2 - \psi_1) & \rho_f (c_f^2 + \psi_2) \end{pmatrix},$$

$$E_0 = \begin{pmatrix} \exp\left(-\frac{\eta_{02} H_0}{c_f}\right) & 0 \\ 0 & \exp\left(-\frac{\eta_{01} H_0}{c_f}\right) \end{pmatrix},$$

$$\psi_1 = \frac{gc_f \eta_{01}}{\omega^2}, \quad \psi_2 = \frac{gc_f \eta_{02}}{\omega^2},$$

$$\eta_{01} = -\omega\gamma - \frac{g}{2c_f}, \quad \eta_{02} = \omega\gamma - \frac{g}{2c_f}.$$

At the other side of this boundary, the solid-liquid interface:

$$\begin{pmatrix} kW \\ \sigma_{zz} \end{pmatrix} = V \begin{pmatrix} C_1 \\ D_1 \\ E_1 \\ F_1 \end{pmatrix}, \quad (14b)$$

where

$$V = \begin{pmatrix} \frac{a_m \alpha_m}{c} & -\frac{a_m \alpha_m}{c} & -\frac{b_m^2}{c^2} & \frac{b_m^2}{c^2} \\ \rho_m \alpha_m^2 \left(1 - \frac{2b_m^2}{c^2}\right) & \rho_m \alpha_m^2 \left(1 - \frac{2b_m^2}{c^2}\right) & \frac{2v\beta_m b_m}{c} & \frac{2v\beta_m b_m}{c} \end{pmatrix}$$

and  $v = \rho_m b_m^2$  ( $m = 1$  for the soft sedimentary layer). To sum up, we have

$$ME_0 \begin{pmatrix} A_0 \\ B_0 \end{pmatrix} = V \begin{pmatrix} C_1 \\ D_1 \\ E_1 \\ F_1 \end{pmatrix}. \quad (14c)$$

Using the condition at the free surface, the two equations represented by (14c) can be reduced to one.

Since fluid can not sustain shearing stress, continuity of the stress at the interface requires that the tangential component of the stress be zero:

$$\begin{pmatrix} -\frac{2a_m\alpha_m}{c} & \frac{2a_m\alpha_m}{c} & \frac{2b_m^2}{c^2} & -1 \\ -\frac{2b_m^2}{c^2} & +1 & & \end{pmatrix} \begin{pmatrix} C_1 \\ D_1 \\ E_1 \\ F_1 \end{pmatrix} = 0. \quad (15)$$

Following the Haskell method again, we construct a matrix that relates the components of motion at one interface in a layered structure to those at the next. For the  $m$ th solid layer, this is as follows:

$$P_m = T_m E_m^{-1} T_m^{-1}, \quad (16)$$

where

$$T_m = \begin{pmatrix} \frac{a_m^2}{c^2} & \frac{a_m^2}{c^2} & -\frac{\beta_m b_m}{c} & -\frac{\beta_m b_m}{c} \\ \frac{\alpha_m a_m}{c} & -\frac{\alpha_m a_m}{c} & -\frac{b_m^2}{c^2} & \frac{b_m^2}{c^2} \\ -\frac{2\mu_m \alpha_m a_m}{c} & \frac{2\mu_m \alpha_m a_m}{c} & \frac{2\mu_m b_m^2}{c^2} - 1 & -\frac{2\mu_m b_m^2}{c^2} + 1 \\ \rho_m a_m^2 \left(1 - \frac{2b_m^2}{c^2}\right) & \rho_m a_m^2 \left(1 - \frac{2b_m^2}{c^2}\right) & \frac{2\nu\beta_m b_m}{c} & \frac{2\nu\beta_m b_m}{c} \end{pmatrix},$$

and

$$E_m = \begin{pmatrix} \exp\left(-\frac{\omega\alpha_m H_m}{a_m}\right) & 0 & 0 & 0 \\ 0 & \exp\left(-\frac{\omega\alpha_m H_m}{a_m}\right) & 0 & 0 \\ 0 & 0 & \exp\left(-\frac{\omega\beta_m H_m}{b_m}\right) & 0 \\ 0 & 0 & 0 & \exp\left(-\frac{\omega\beta_m H_m}{b_m}\right) \end{pmatrix}$$

At the  $m$ -interface, between the  $m$ th and  $m + 1$ th layers, the condition of motion continuity is

$$T_m E_m \begin{pmatrix} C_m \\ D_m \\ E_m \\ F_m \end{pmatrix} = T_{m+1} \begin{pmatrix} C_{m+1} \\ D_{m+1} \\ E_{m+1} \\ F_{m+1} \end{pmatrix}. \quad (17)$$

Subsequently, with the application of (17), we obtain the expression that relates the coefficients in the first solid layer to those in the half-space (last solid layer):

$$\begin{pmatrix} C_1 \\ D_1 \\ E_1 \\ F_1 \end{pmatrix} = T_1^{-1} P_2 \dots P_{n-1} T_n \begin{pmatrix} C_n \\ E_n \end{pmatrix}, \quad (18)$$

where

$$T_n = \begin{pmatrix} \frac{a_m^2}{c^2} & -\frac{\beta_m b_m}{c} \\ \frac{\alpha_m a_m}{c} & -\frac{b_m^2}{c^2} \\ -\frac{2\mu_m \alpha_m a_m}{c} & \frac{2\mu_m b_m^2}{c^2} - 1 \\ \rho_m a_m^2 \left(1 - \frac{2b_m^2}{c^2}\right) & \frac{2\nu\beta_m b_m}{c} \end{pmatrix}$$

represents the matrix for the half-space.

Expressions (15) and (18) can now be used to determine the displacement coefficients in the half-space. To find the coefficients of the eigenfunctions in the liquid layer, we need to start with the expression for the pressure vanishing at the free surface.

The characteristic function, which represents a function of phase velocity, wavenumber, and the elastic constants of the layer, can now be easily obtained using the final product of the layer matrix multiplication as well as the conditions of vanishing normal stress at the free surface and tangential stress at the liquid-solid boundary. We do not describe this procedure in detail here, since this has previously been well documented by numerous other investigators (Press *et al.*, 1961; Aki and Richards, 1980; Shearer, 1999; Udias, 1999).

### Tsunami and Rayleigh Waves from Point and Distributed Source

To derive the expression for the displacement of a stationary surface wave excited by a point source in the homogeneous half-space, we follow the theory of surface waves in the vertically inhomogeneous media developed by Levshin (1978) and Keilis-Borok (1989). It is based on the expansion of the solution into eigenfunctions of the boundary problem. In the context of this approach, the spectrum of displacement in an interference wave (Rayleigh and Love) can be expressed as a product of four factors. The first is the complex constant, while the second describes the effect of geometric divergence of the energy flow on the wave propagation. The third term depends on the depth of the receiver, and the final one depends on the source parameters, that is, on depth, focal mechanism, and the radiation spectrum. In the far-field approximation of this theory, the expression of displacement in a surface wave generated by the point source at the depth  $h$  in the solid Earth is the following:

$$u(r, \varphi, \omega, t) = \frac{\exp(-i\pi/4)}{\sqrt{8\pi}} \frac{\exp(i\omega(t-r/c))}{\sqrt{\omega r/c}} \frac{U(z, \omega)}{\sqrt{cuI_0}} \frac{Q(h, \varphi, \omega)}{\sqrt{cuI_0}}; \quad (19)$$

where  $U(z, \omega) = U(z, \omega)e_r + W(z, \omega)e_z$ ,  $Q(h, \varphi, \omega) = m_{rs}(\omega)B_{rs}(h, \varphi, \omega)$  is the excitation function;  $m_{rs}(\omega)$  is the spectrum of the seismic moment tensor; and  $B_{rs}(h, \varphi, \omega)$  is a tensor that can be expressed via the eigenfunctions

$U(z, \omega)$  and  $W(z, \omega)$  and their derivatives and that depends on the axis orientation of the source. Also,  $I_0 = \int_0^\infty \rho [U^2(z, \omega) + W^2(z, \omega)] dz$  represents the energy;  $u$  is the group velocity.

Only three basic seismic mechanisms, specifically a strike-slip earthquake on a vertical fault, a dip-slip earthquake on a vertical fault, and pure thrusting on a fault dipping  $45^\circ$  are considered in the present study. The reason for this is that any other double-couple mechanism can be obtained as a linear superposition of these mechanisms (Okal, 1988).

We follow the analysis of the surface-wave excitation terms as given by Levshin (1978).

#### Dip-Slip Source

Let the fault plane be orthogonal to the  $x$  axis and the displacement be vertical. Then the seismic moment tensor has two nonzero components:

$$m_{xz} = m_{zx} = M_0 F(\omega), \quad (20)$$

where  $M_0$  is the seismic moment and  $F(\omega)$  is the seismic moment spectrum. The corresponding components of tensor  $\mathbf{B}$  are expressed in the form (Keilis-Borok, 1989)

$$B_{xz} = B_{zx} = \frac{i \cos \varphi}{2} \left( -\xi W_2 + \frac{dU_2}{dz} \right), \quad (21)$$

where  $\xi = \omega/c$  is the wavenumber.

Thus,

$$Q(h, \omega, \varphi) = iM_0 \cos \varphi \left( -\xi W_2 + \frac{dU_2}{dz} \right) F(\omega); \quad (22)$$

and

$$q(h, \omega, \varphi) = \frac{i \cos \varphi \left[ -\xi W_2(h, \omega) + \frac{dU_2(z, \omega)}{dz} \Big|_{z=h} \right]}{\sqrt{cul_0}}. \quad (23)$$

In the case of  $45^\circ$  -dip thrust - $m_{yy}$  and  $m_{zz}$  the moment tensor components are non-zero. This yields the excitation function:

$$q(h, \omega, \varphi) = \frac{\left[ \cos^2 \varphi \xi U_2(h, \omega) + \frac{dW_2(z, \omega)}{dz} \Big|_{z=h} \right]}{\sqrt{cul_0}}. \quad (24)$$

Formula (25), from Ben-Menahem (1964), can be used to compute the excitation term for thrust events with arbitrary dip angle.

To estimate source radiation function, some value of the seismic moment  $M_0$  and its spectrum  $F(\omega)$  must be assumed. We assume values of the radiation function up to the factor  $M_0$  and for the azimuth along which seismic radiation is maximal. Thus,

$$F(\omega) = \frac{1}{i\omega(i\omega\tau_0 + 1)}, \quad (25)$$

where  $\tau_0$  is the rise time.

#### Strike-Slip Source

The fault is assumed to be the same as in the former case, but the slip occurs along the  $y$  axis. In this case the nonzero components of the moment tensor are

$$m_{xy} = m_{yx} = M_0 F(\omega)$$

and the corresponding components of the tensor  $\mathbf{B}$  are as follows:

$$B_{xy} = B_{yx} = -\frac{\omega}{2c} U_2 \sin 2\varphi.$$

The source function  $Q$  is then:

$$Q(h, \omega, \varphi) = -M_0 \frac{\omega}{c} U_2 \sin 2\varphi \cdot F(\omega).$$

$$q(h, \omega, \varphi) = -\frac{\xi U_2(h, \omega) \sin 2\varphi}{\sqrt{cul_0}} \quad (26)$$

To bring more realism into the tsunami and Rayleigh-wave generation process, as well as to study the tsunami-earthquake events, we use the finite dimensional line source. This can be modeled by a set of point sources, uniformly distributed along the fault and moving along it at a constant velocity. We consider the case where the fault length is much greater than its width (in other words, we neglect the two-dimensionality of the fault).

With the relation between the moment tensor ( $\mathbf{M}$ ) and the moment density tensor ( $\mathbf{m}$ ) in the form

$$M_{pq} = \int_L m_{pq} dL \quad (27)$$

the normalized excitation function in the case of the finite dimensional line source becomes

$$\begin{aligned} \frac{\hat{Q}(h, \omega, \varphi)}{\sqrt{cul_0}} &= \int_0^{L_0} \mathbf{m}(\omega, L) \exp \left[ -i\omega L \left( \frac{1}{V} - \frac{\cos \alpha}{c} \right) \right] \\ &\times \frac{Q(h^1, \omega, \varphi)}{\sqrt{cul_0}} dL, \end{aligned} \quad (28)$$

where  $h^1 = h_0 - L \sin \alpha$  is the depth of the moving point  $L_0$  at the fault;  $\mathbf{m}$  is the seismic moment density  $\int_0^{L_0} \mathbf{m}(\omega, L) dL = M_0(\omega)$ ;  $L_0$  is the fault length;  $V$  is the velocity of the rupture propagation;  $c$  is the phase velocity;  $\alpha$  is the azimuth of the station measured from the rupture direction; and  $L(1/V - \cos \alpha/c)$  is the rupture time.

Given that the earthquake rupture velocity  $V$  is typically about  $80\% \pm 10\%$  of the shear velocity according to the standard definitions of seismic moment along with the em-

pirical observations (Bilek and Lay, 1999), formula (28) can be rewritten in the following form:

$$\frac{Q(h, \omega, \varphi)}{\sqrt{cuI_0}} = \int_0^{L_0} \mathbf{m}(\omega, L) \exp \left[ -i\omega L \left( \frac{1}{0.8\sqrt{\mu/\rho}} - \frac{\cos\alpha}{c} \right) \right] \times \frac{Q(h^1, \omega, \varphi)}{\sqrt{cuI_0}} dL, \quad (29)$$

where  $\mu$  and  $\rho$  are the rigidity and rock density, respectively.

### Results and Discussion

Mooney *et al.* (1998) have pointed out that when thickness of oceanic sediments exceeds 2 km (such as in oceanic trenches), it is necessary to use a model with two layers of sediments to justify a detailed description of variations in their physical properties.

Taking into account the model proposed by Mooney with two low-rigidity layers, we describe the tsunami excitation in the area with thick accumulation of sediments

(Yoshii *et al.*, 1970; Westbrook *et al.*, 1973). The parameters of the model for each numerical experiment are given in the Table 1.

### Tsunami Waves

Figure 2a and b shows the dependence of phase and group velocities on period for various models of an oceanic structure. For small periods, both velocities decrease rapidly with period. This corresponds to the case with gravity waves in deep water ( $kH \gg 1$ ). An interval of periods greater than 200 sec, when the phase velocity is period independent, corresponds to gravity waves (tsunami) in shallow water ( $kH \ll 1$ ). Obviously, the presence of sedimentary layers has no effect on tsunami-wave propagation. This is understandable because during propagation, the main effect is due to the influence of both the gravity forces in a liquid and the parameters of the liquid ( $c = \sqrt{gH}$ ). The parameters of the half-space and its layered structure have no influence at all on the wave velocities.

To study how the sediments exert on the tsunami excitation process, we place a point source at various depths in a layered half-space. For investigation, we choose three

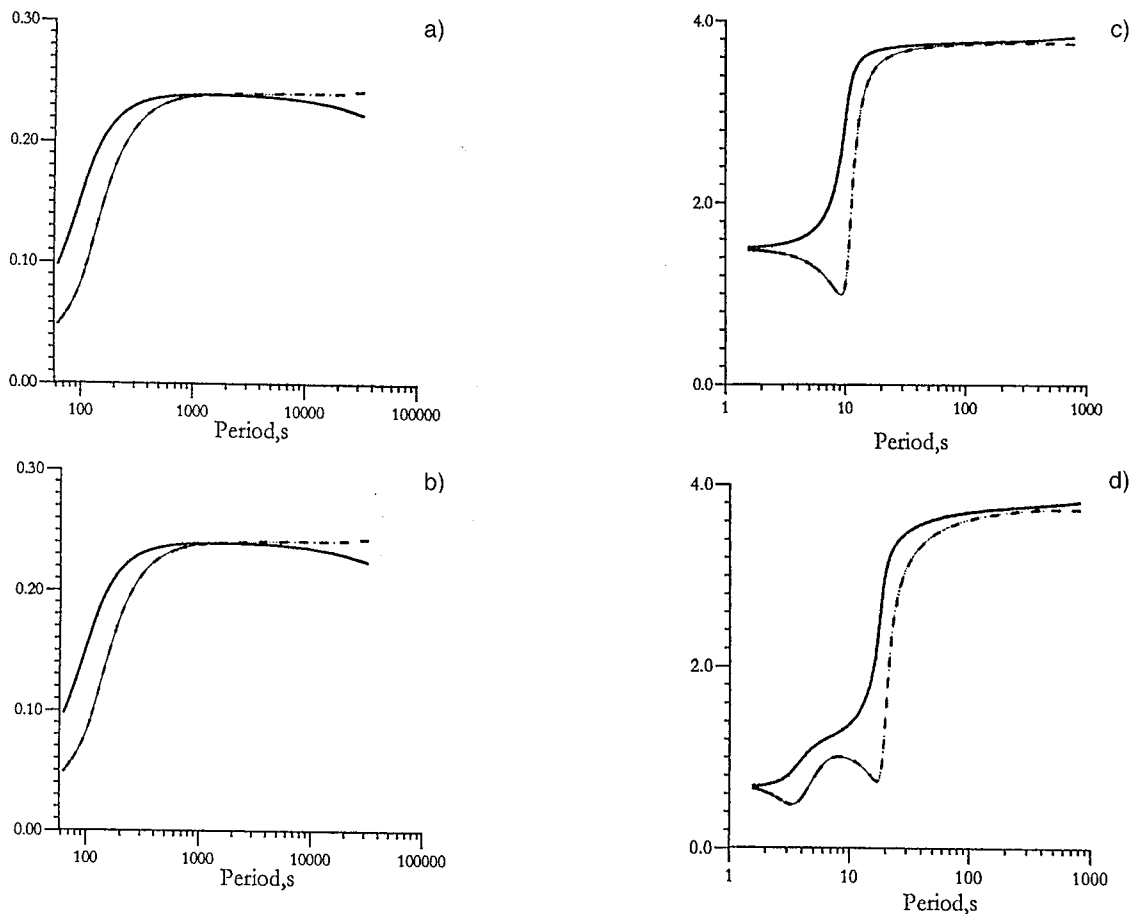


Figure 2. Phase (solid line) and group (dashed line) velocities of tsunami (a,b) and Rayleigh (c,d) waves in the liquid half-space model (a,c) and liquid-layered half-space model (b,d).

basic geometries of the source: dip-slip, 45°-thrust, and strike-slip.

Figures 3–5 show the behavior of the 45°-thrust (3a–5a), dip-slip (3b–5b) and strike-slip (3c–5c) excitation functions of the gravity waves at various source locations in the layered half-space, starting with the position at  $z = 6.5$  km in the soft sediments. The intensity of the excitation function maximum decreases by one order of magnitude when the source is displaced from soft into hard sediments and by the same factor with further deepening of the source into the basement. Such a sharp decrease is mainly caused by an increase in rock rigidity with depth rather than with a mere deepening of the source. The most effective tsunami-exciting source is the fault with thrust motion (Okal, 1988), as tsunamis from this source are one order of magnitude greater than those from the other sources. This feature is also re-

vealed in calculated theoretical marigrams (Figs. 3d–f; 4d–f, and 5d–f).

To ensure that it is the rock rigidity that exert the strongest influence on tsunami excitation, we carried out our computations for a simple liquid layer–elastic half-space model. We calculated tsunami synthetics for two locations of seismic source in half-space: 6.5 km (this depth corresponds to the source location in soft sedimentary layer in previous experiment) and 9 km (this corresponds to the source position in hard sedimentary layer in previous experiment). Obviously, the amplitude of a tsunami wave from a source located in half-space at the 6.5-km depth (Fig. 6a) and at the 9-km depth (Fig. 6b) is over one order of magnitude less than the tsunami amplitude in the case of layered model, when a source is located either in soft (Fig. 3d–f) or in hard sediments (Fig. 4d–f). The distinctive peculiarity of tsunami-

Table 1  
Parameters of the Model

Liquid Layer	$cf = 1.45$ km/sec; $\rho_1 = 1.0$ g/cm <sup>3</sup> ; $H = 6.0$ km
Soft sedimentary layer	$V_p = 1.77$ km/sec; $V_s = 0.8$ km/sec; $\rho_2 = 1.9$ g/cm <sup>3</sup> ; $h_1 = 1.0$ km
Hard sedimentary layer	$V_p = 3.9$ km/sec; $V_s = 2.3$ km/sec; $\rho_3 = 2.5$ g/cm <sup>3</sup> ; $h_2 = 5.0$ km
Elastic half-space	$V_p = 7.15$ km/sec; $V_s = 4.1$ km/sec; $\rho_3 = 3.1$ g/cm <sup>3</sup>

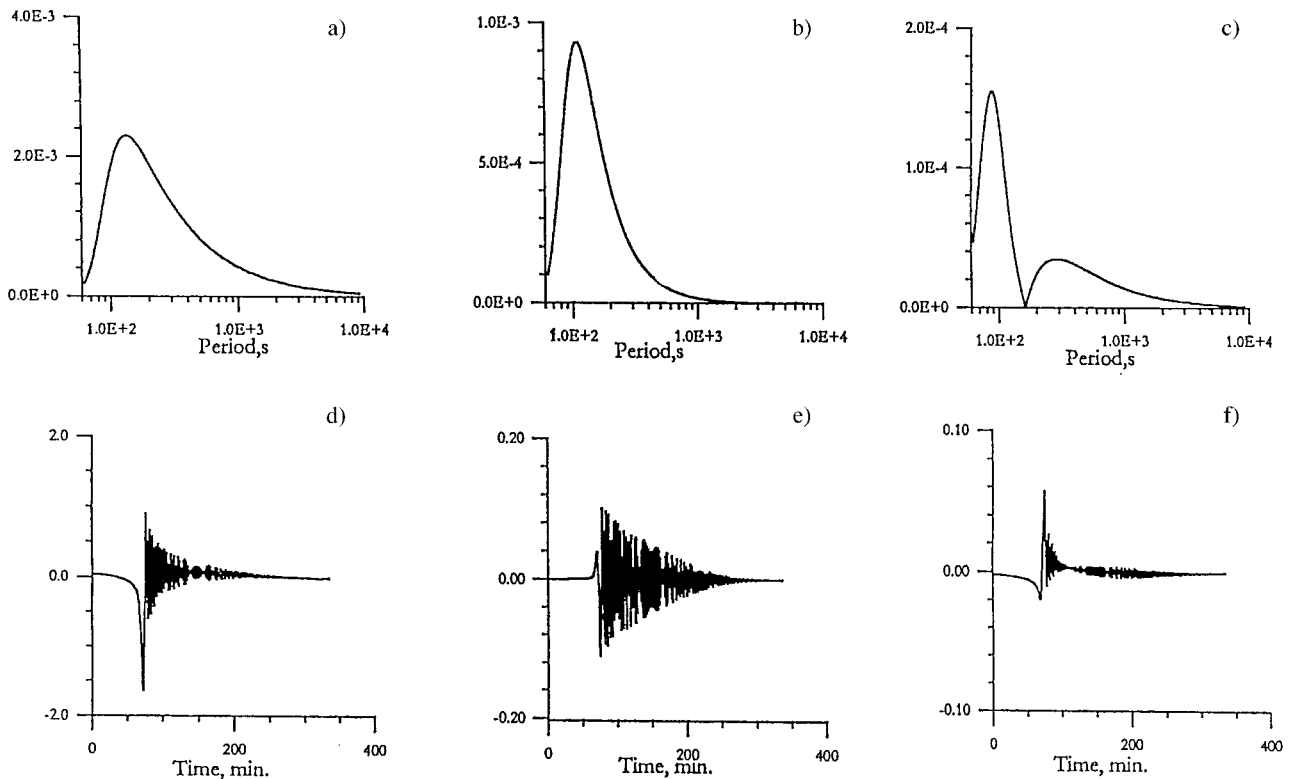


Figure 3. Functions  $|q(h, \omega, \phi)|$  versus period for (a) 45°-thrust, (b) dip-slip, (c) strike-slip seismic sources located in the soft sedimentary layer at  $z = 6.5$  km and theoretical marigrams (d–f) of tsunami wave (vertical component) at the 1000 km distance from the above sources.

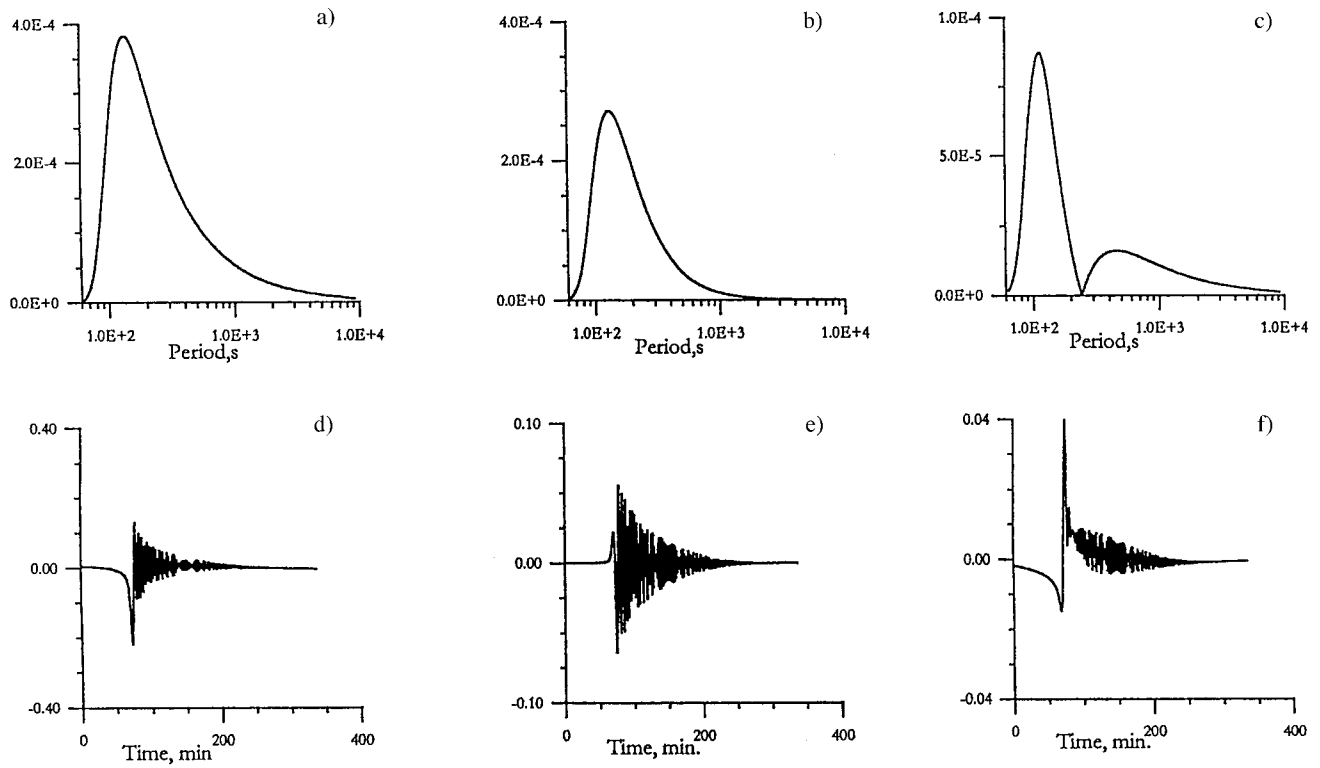


Figure 4. The same as in Figure 3, but for the source location in the hard sedimentary layer ( $z = 9$  km).

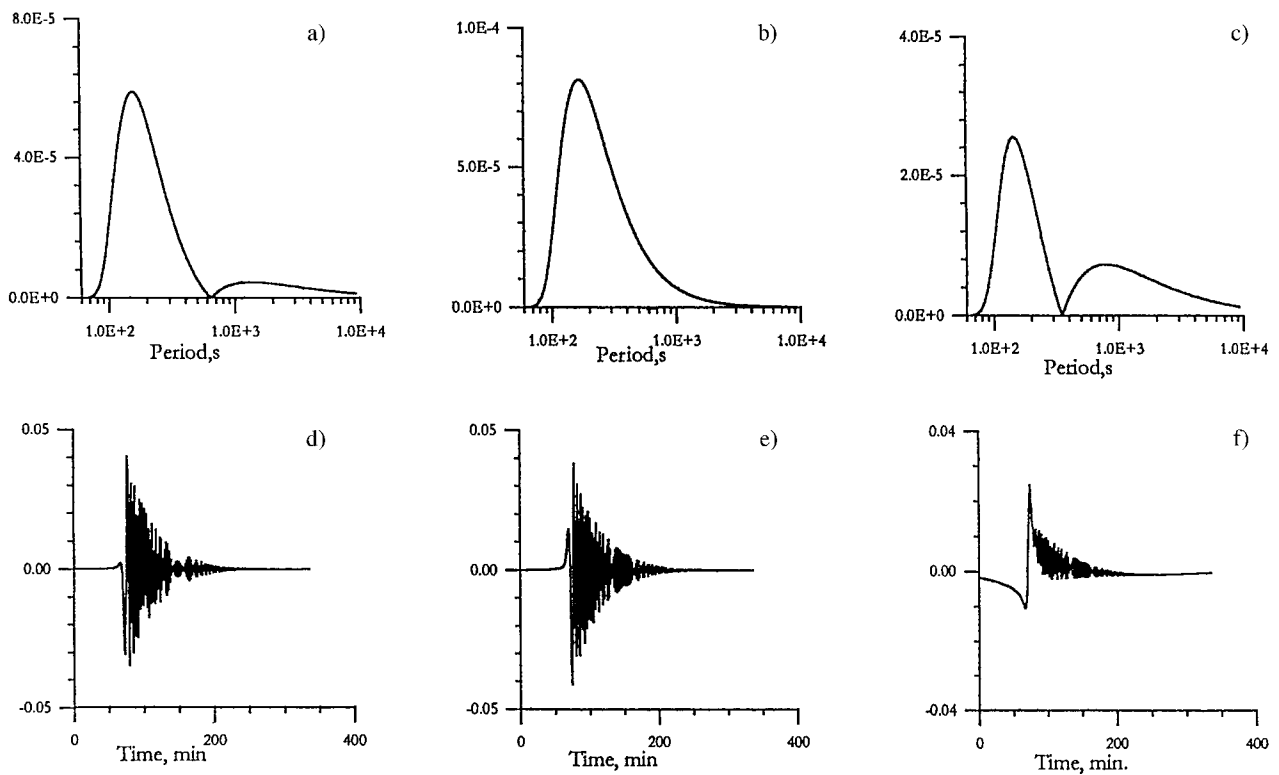


Figure 5. The same as in Figures 3 and 4, but for the source location in the half-space ( $z = 15$  km).

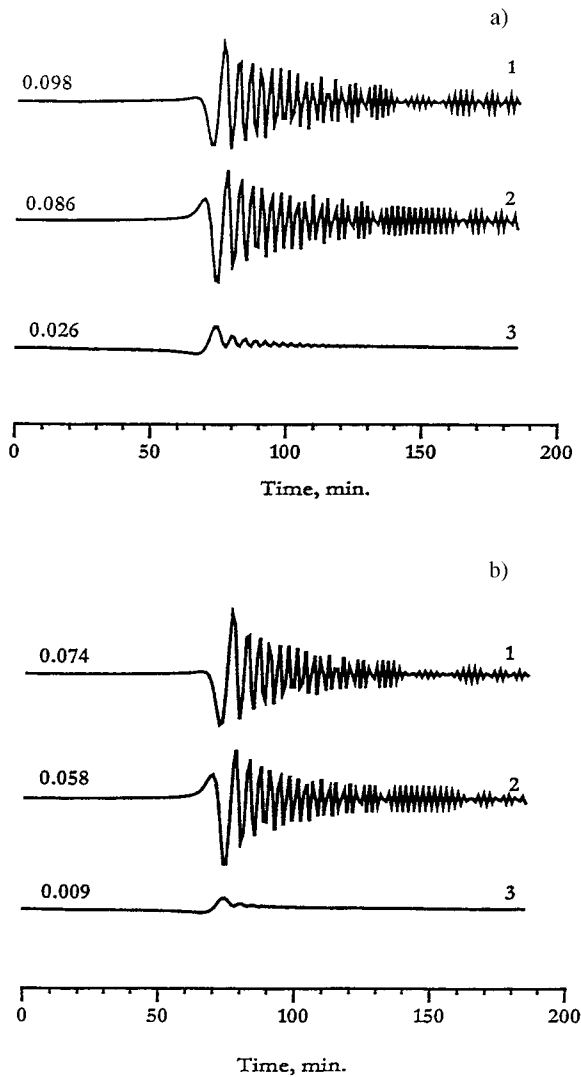


Figure 6. Theoretical marigrams of tsunami wave at the 1000-km distance from the source located in the half-space at (a) 6.5-km depth and at (b) 9 km.

wave behavior is that dip-slip and 45°-thrust sources located in elastic half-space (for the liquid layer–half-space model) generate a wave of almost the same magnitude as compared with the case of dip-slip and 45°-thrust sources located at the same depths, but in soft and in hard sediments (for the layered model).

### Rayleigh Waves

Figures 2c and 2d show the dispersion curves of the fundamental mode of Rayleigh wave in the liquid half-space model and in the liquid-layered half-space model, respectively. Unlike gravity waves, Rayleigh waves show a strong dependence on a layered structure along the propagation path, especially in the 1- to 10-sec period range. The reason is that in the case of Rayleigh waves, the restoring force is elastic, not gravitational, and therefore the elastic parameters

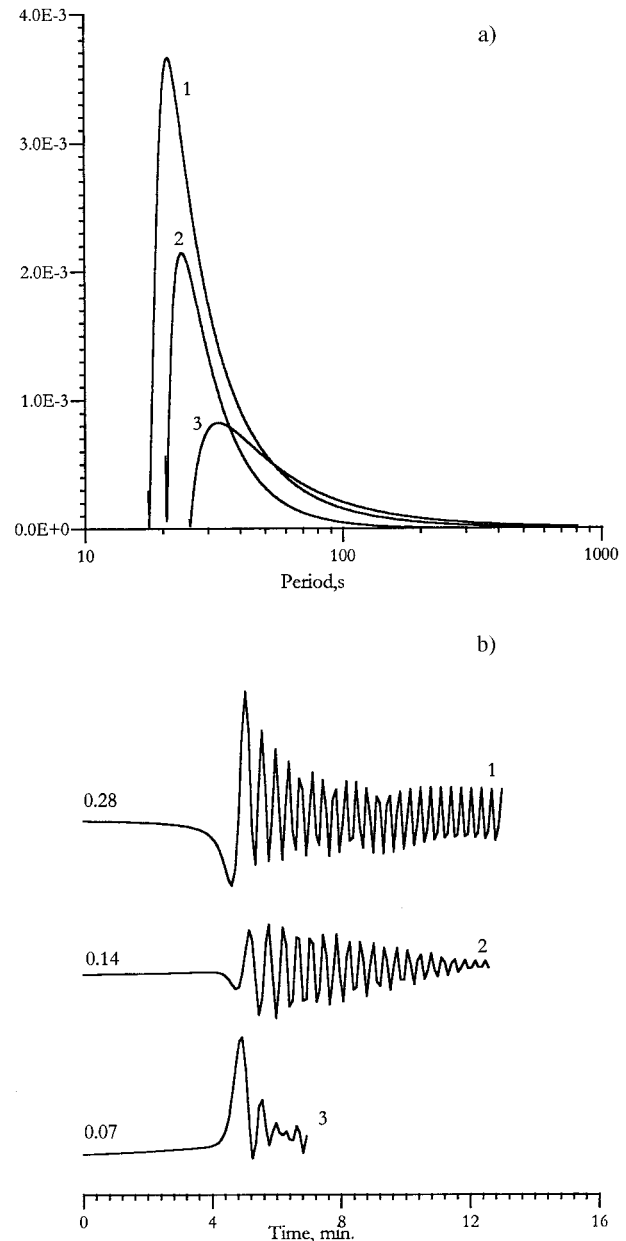


Figure 7. Rayleigh-wave excitation functions (a) for strike-slip (curve 1), dip-slip (curve 2), and 45°-thrust (curve 3) point sources, located in the hard sediments ( $z = 9$  km), and (b) synthetics at the 1000-km epicentral distance from the aforementioned sources. The numbers at the left side indicate the wave amplitude in cm.

at the bottom along with the layered structure significantly affect the wave propagation.

Figure 7 shows the excitation function of the fundamental Rayleigh wave (Fig. 7a) and synthetics (Fig. 7b) at the 1000-km epicentral distance. Evidently the thrust seismic source, which is located shallow in the sedimentary layer, generates a wave that is approximately 2 times weaker (curve 3, Fig. 7b) than other types of seismic sources such

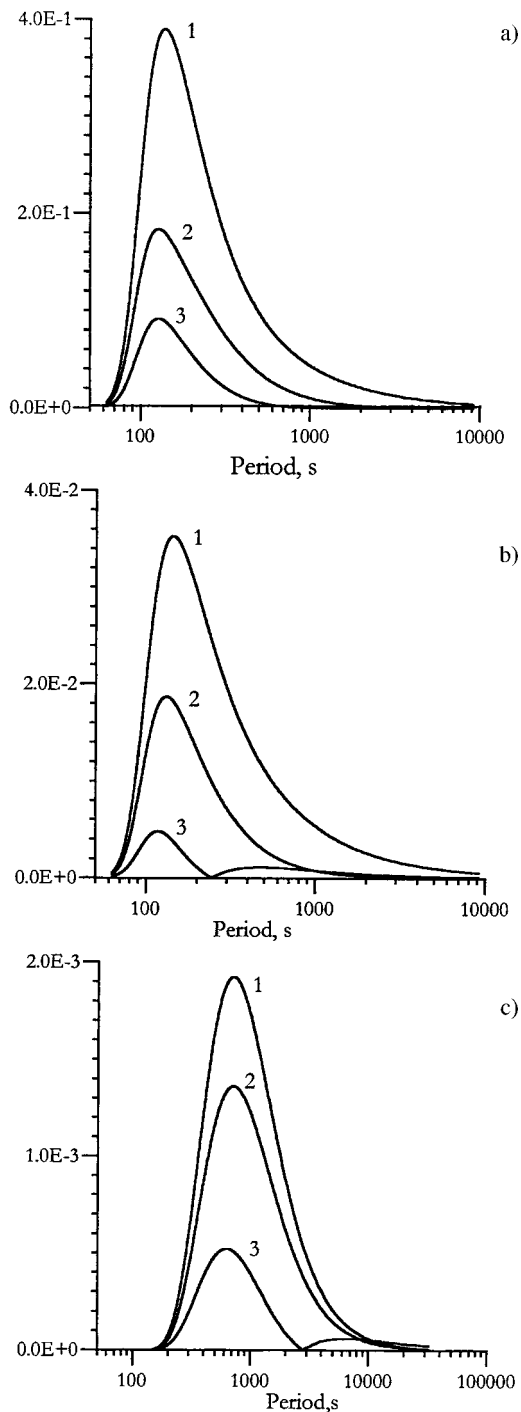


Figure 8. Tsunami-wave excitation functions from 45°-thrust (curves 1), dip-slip (curves 2), strike-slip (curves 3) distributed seismic sources located in the (a) soft sedimentary layer, (b) hard sedimentary layer, and (c) half-space.

as dip-slip (curve 2) and strike-slip (curve 1) sources, which are more or less equally effective in Rayleigh-wave excitation.

From excitation function behavior, one would expect that amplitude of Rayleigh wave should be higher, but from

the synthetics we could not obtain that. The reason is that oceanic surface waves of this type with predominant periods of 10 to several tens of seconds are very sensitive to the rise-time variation: as the rise time increases the contribution to wave amplitude decreases.

#### Numerical Modeling of Tsunami and Tsunamigenic Earthquakes

It is well known (Houston, 1999) that the rigidity of a rock, in which a seismic rupture occurs, controls the amount of slip in an earthquake of a given size and should therefore exert a strong influence on the size of tsunamis generated by an underwater rupture. For a lower rigidity, an underwater rupture of a given seismic moment can generate larger slip or surface area of slippage and thus a larger tsunami.

Taking this into account, we analyze an earthquake fault rupturing in structures with different rigidities. First of all, for numerical modeling of tsunami-earthquakes we choose the distributed model of the seismic source. To take realistic earthquake parameters, we analyze several typical events of this class. Among these are the 1896 Sanriku, 1946 Aleutian, 1960 Peru, 1963 Kurile, and 1992 Nicaragua events. These are thrust-faulting events of long source duration (85–130 sec), very shallow fault dip (6°–8°), and shallow source depth ( $h = 5$ –10 km). Based on that, for the numerical experiment we take the 6°-dip thrust fault with 100-km length, located at  $h = 6.5$  km in a sedimentary layer. To study the influence of source duration on the wave amplitude, we vary the rigidity of the structure (Fig. 8a,b). Evidently, any of the considered seismic sources located in soft sediments (Fig. 8a) is able to generate a stronger tsunami wave compared to those located in hard sediments (Fig. 8b). This result is strongly supported by the observation fact that the seismic source that ruptured in a low-rigidity media is usually characterized by a long duration and produces a larger tsunami (Pelayo and Wiens, 1992).

Figure 9 represents examples of Rayleigh (Fig. 9a,b) and seismic sea waves (Fig. 9c,d) synthetics for a tsunami-earthquake. Amplitude of tsunami from a thrust fault is twice as large as one from a dip-slip earthquake, and one order of magnitude larger than one from a strike-slip. Shallow thrust events, ruptured in the sedimentary layer, generate relatively weak seismic waves. Rayleigh waves (curves 3 in Fig. 9a and b) from the source with such mechanism are more than one order of magnitude weaker compared to the tsunami. This agrees well with the observational data.

To study the behavior of oceanic surface waves with distance, we calculate marigrams for two different epicentral distances:  $r = 300$  and 1000 km. Figures 9c and 10a show that tsunami amplitude is 2.5 times greater at 300 km away from the source than at 1000 km away (Figs. 9d, 10b). It corroborates the observation fact that sea waves from tsunami earthquakes mainly affect coastal regions close to a source area. However, tsunamis from thrust events can still reach strong-enough amplitudes up to 2 m—even at a 1000-

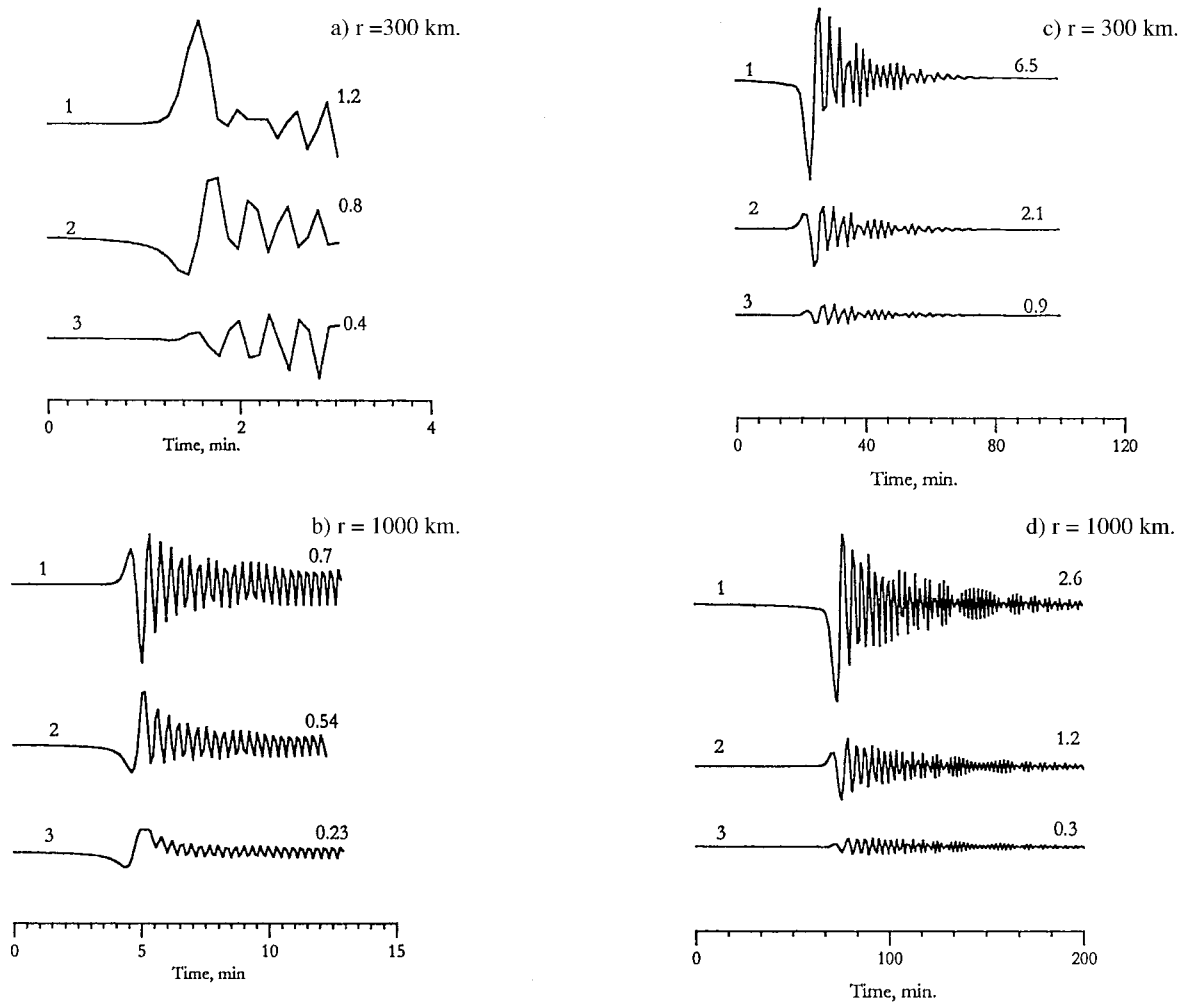


Figure 9. (a,b) Rayleigh and (c,d) tsunami wave synthetics at 300 and 1000 km away from a distributed seismic source located in soft sediments. For the tsunami, curve 1 corresponds to the thrust event, curve 2 to the dip-slip event, and curve 3 to the strike-slip. For the Rayleigh-wave, curve 1 corresponds to the strike-slip event, curve 2 to the dip-slip event, and curve 3 to the thrust event. In both cases right side numbers indicate the wave amplitude in m.

km epicentral distance. Comparative analysis of the tsunami-wave synthetics (Figs. 9c,d and 10) computed for models with different parameters of low-rigidity layers shows that the rigidity of the rocks exerts a strong influence on the velocity of rupture propagation and consequently on the source duration. These factors strongly affect the wave amplitude. To prove this additionally we carried out calculations of tsunamis for the simple liquid layer–elastic half-space model. In these calculations we used the same models of a distributed source located in half-space. The comparison of Figures 9c,d and 11a,b shows that the difference in amplitude of the tsunami wave from the source located in the soft sedimentary layer (for the layered model) is more than one order of magnitude greater than that from the source located at the same depth in elastic half-space, but for the liquid–half-space model.

Using the distributed models of different seismic

sources, we also make a comparative analysis as to what type of source is most dangerous from the point of view of tsunami excitation (Fig. 8c). We carry out computations for typical large tsunamigenic events (such as the 1929 Fox Islands, 1938 Alaskan, 1965 Rat Islands) with the 100-km length and rupture velocity of  $\sim 3.3$  km/sec. From observations, it is well known that such earthquakes with seismic moment  $M_0 \sim 6.5 \times 10^{27}$  dyne cm or greater are usually located at depths between 15 and 50 km. Accordingly we place a seismic source with the aforementioned parameters in a hard-rock half-space (Fig. 8c). It appears that  $45^\circ$ -deep-thrust (curve 1) and dip-slip (curve 2) earthquakes are more or less capable of exciting a tsunami. A distributed source with strike-slip motion generates less-intensive waves (curve 3). Tsunami synthetics computed at the 300- (Fig. 12a) and 1000-km (Fig. 12b) epicentral distances also confirm this. These theoretical results are consistent with the observed

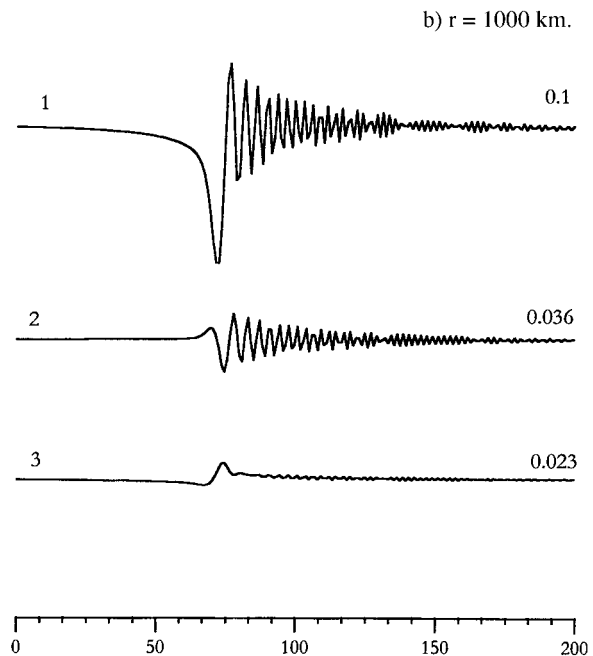
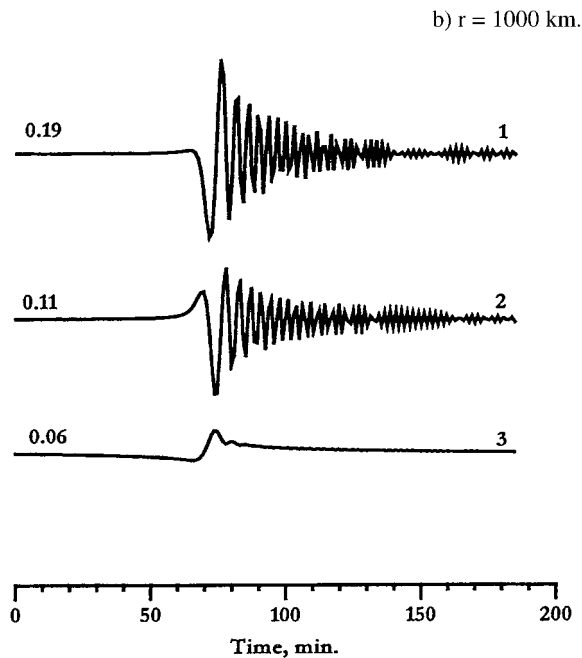
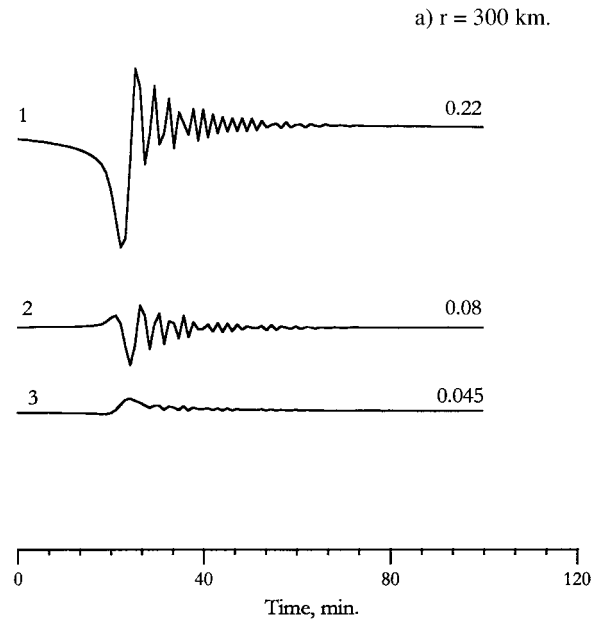
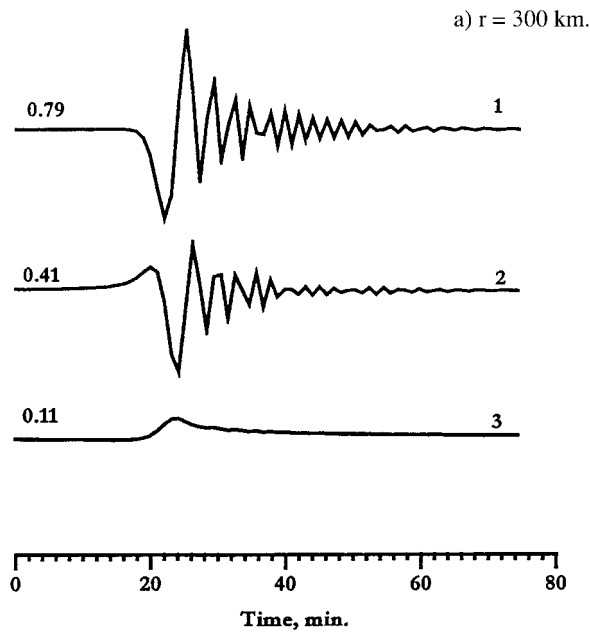


Figure 10. Comparison of theoretical marigrams of the tsunami wave at (a) 300 km and (b) 1000 km from the distributed seismic source located in hard sediments. The numbers at the left hand side of the figures indicate the wave amplitude in m. For both cases curve 1 corresponds to the thrust event, curve 2 to the dip-slip event, and curve 3 to the strike-slip events.

Figure 11. Theoretical marigrams of the tsunami wave at the (a) 300 km and (b) 1000 km from the distributed seismic source located in half-space (liquid layer-elastic half-space model). The numbers at the right-hand side of the figures indicate the wave amplitude in m. For both cases, curve 1 corresponds to the thrust event, curve 2 to the dip-slip event, and curve 3 to the strike-slip events.

facts that strong tsunamigenic earthquakes, such as those in Niigata (16 June 1964), Akita-Oki (7 May 1964), Sakhalin (6 September 1971) and in the Central Japan Sea (26 May 1983) were mostly dip-slip and thrust events.

## Conclusions

This article presents an analytical model for investigation of excitation and propagation of tsunami and oceanic Rayleigh waves in the multilayered ocean-Earth structure.

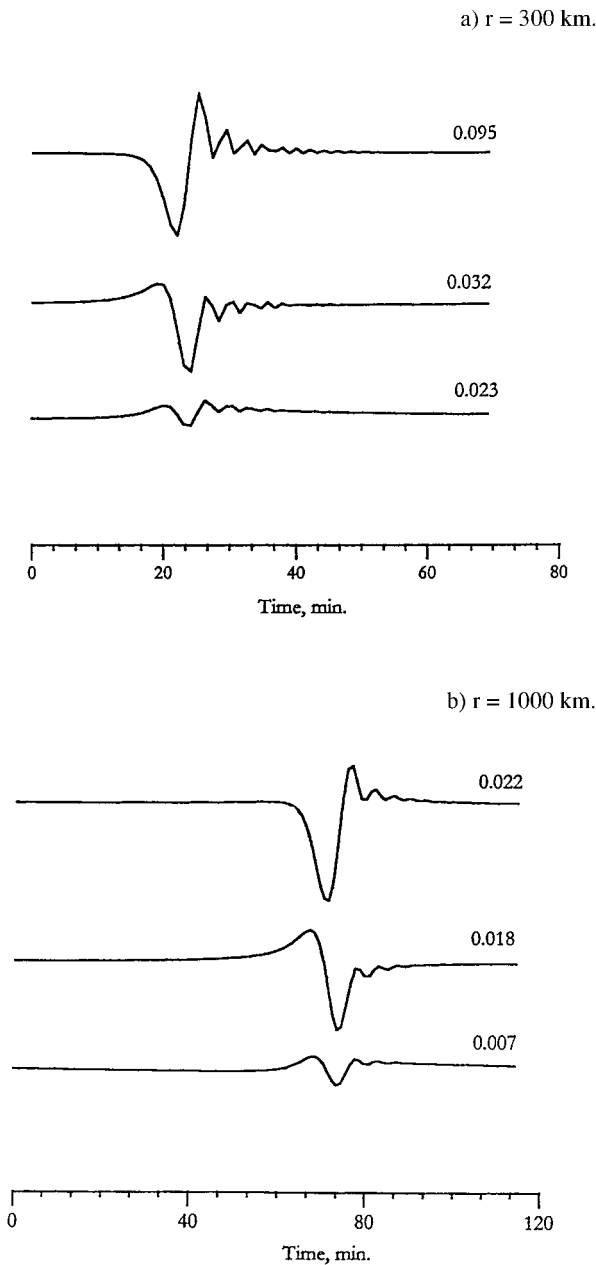


Figure 12. The same as in Figure 10, but for the source located in half-space.

Applying the far-field approximation of the normal mode theory allows us to analyze the aforementioned processes separately.

We observed the following features of the tsunami and Rayleigh-wave behavior:

1. A low rigidity of sediments and a layered structure of the ocean bottom have no effect on tsunami propagation. However, sedimentary layers strongly affect the excitation process of tsunami waves: the most strongest tsunamis are generated by thrust events ruptured within the soft sedimentary layer. Excitation intensity decreases rap-

idly not only with a mere deepening of source but mainly because the rock rigidity increases with depth. It was strongly supported by numerical calculations for both layered and simple liquid–elastic half-space models. According to our results, the amplitude of the tsunami wave from any type of seismic source located in the half-space (for the liquid half-space model) is over one order of magnitude less than the tsunami amplitude in the case of layered model, when a source is located at the same depth either in soft or in hard sediments.

2. Dispersion of Rayleigh waves strongly depends on the layered character of the ocean bottom, especially in the 1- to 20-sec period range.
3. The synthetics of seismic sea and Rayleigh waves have been computed, and comparative analysis has been carried out for both tsunami and tsunamigenic events. Using the normal mode formalism, we show that tsunami amplitude in the region that is respectively close to the source area is 2.5 times greater than in the region 1000 km away from source. Unlike previous studies, we find that sea-wave amplitude from tsunami earthquakes is still strong enough (around 2 m) even at a 1000-km distance from the epicentral area. One would expect a much larger increase in tsunami amplitude in both near- and far-field zones if the actual bathymetry is incorporated into the present model. Being located in soft sediments, a thrust event evidently generates a far stronger tsunami than either a dip-slip or strike-slip event, and a weak surface wave of Rayleigh type. For typical tsunamigenic earthquakes at depths between 15 and 50 km, dip-slip and thrust events are more or less just as effective with respect to tsunami excitation.

The analytical model developed in the present study allows previously obtained results for tsunami and Rayleigh-wave excitation and propagation in the simple liquid half-space model to be applied to a more realistic ocean-crust structure. Our attempt to model tsunami and Rayleigh-wave generation and propagation can hopefully contribute to the theoretical aspect of the major problem in real-time tsunami warning: recognizing an anomalous event such as a tsunami earthquake.

From the practical point of view, study of tsunami earthquakes as tectonically significant events is very important in terms of long-term prediction of great earthquakes because the distribution of low-frequency earthquakes in space and time can be affected by great earthquakes occurring near oceanic trenches (Utsu, 1980).

### Acknowledgments

This research was supported by a grant from the Institute of Earth Sciences of Academia Sinica, Taiwan. The authors would like to thank an anonymous reviewer for suggestions that helped to improve an original version of the manuscript.

## References

- Aki, K., and G. Richards (1980). *Quantitative Seismology*, Vol. 1, W. H. Freeman, San Francisco.
- Alexeev, A., and V. Gusiakov (1974). Numerical modeling of tsunami and seismic surface wave generation by a submarine earthquake, in *Tsunami Research Symposium, Bull. R. Soc. N. Z.* **15**, 243–251.
- Ben-Menahem, A., and D. B. Harkrider (1964). Radiation patterns of seismic surface waves from buried dipolar point sources in a flat stratified Earth, *J. Geophys. Res.* **69**, 2605–2620.
- Bilek, S., and T. Lay (1999). Rigidity variations with depth along interplate megathrust faults in subduction zones, *Nature* **400**, 443–446.
- Comer, R. (1984a). The tsunami mode of a flat earth and its excitation by earthquake sources, *Geophys. J. R. Astr. Soc.* **77**, 1–27.
- Comer, R. (1984b). Tsunami generation: a comparison of traditional and normal mode approaches, *Geophys. J. R. Astr. Soc.* **77**, 29–41.
- Dorman, J. (1962). Period equation for waves of the Rayleigh type on a layered, liquid-solid half-space, *Bull. Seism. Soc. Am.* **52**, 389–397.
- Dorman, J., Ewing, M., and J. Oliver (1960). Study of shear-velocity distribution in the upper mantle by mantle Rayleigh waves, *Bull. Seism. Soc. Am.* **50**, 87–115.
- Fukao, Y. (1979). Tsunami earthquake and subduction processes near deep-sea trenches, *J. Geophys. Res.* **84**, 2303–2314.
- Gilbert, F., and G. E. Backus (1966). Propagator matrices in elastic wave and vibration problems, *Geophysics* **31**, 326–332.
- Gusiakov, V. (1975). Excitation of tsunami and oceanic Rayleigh waves by a submarine earthquake, in *Mathematical Problems In Geophysics*, Novosibirsk, Russia, 250–267.
- Harkrider, D. (1964). Surface waves in multilayered elastic media. 1. Rayleigh and Love waves from buried sources in a multilayered elastic half-space, *Bull. Seism. Soc. Am.* **54**, 627–679.
- Haskell, N. A. (1953). The dispersion of surface waves on multilayered media, *Bull. Seism. Soc. Am.* **43**, 17–34.
- Haskell, N. A. (1964). Radiation pattern of surface waves from point sources in a multilayered medium, *Bull. Seism. Soc. Am.* **54**, 377–393.
- Houston, H. (1999). Slow rupture, roaring tsunamis, *Nature* **29**, no. 400, 409.
- Hwang, L.-S., Butler, H. L., and D. Divoky (1972). Tsunami model: generation and open-sea characteristics, *Bull. Seism. Soc. Am.* **62**, 1579–1596.
- Imamura, F., Gica, E., Takahashi, To., and N. Shuto (1995). Numerical simulation of the 1992 Flores tsunami: interpretation of tsunami phenomena in the Northeastern Flores Island and damage at Babi Island, *Pure Appl. Geophys.* **144**, 555–569.
- Kanamori, H. (1972). Mechanism of tsunami earthquakes, *Phys. Earth Planet. Interiors* **6**, 346–359.
- Kanamori, H., and M. Kikuchi (1993). The 1992 Nicaragua earthquake: a slow tsunami earthquake associated with subducted sediments, *Nature* **361**, no. 25, 714–716.
- Keilis-Borok, V. (1989). *Seismic Surface Waves in a Laterally Inhomogeneous Earth*, Kluwer Academic Publishers, Hingham, Massachusetts.
- Knopoff, L. (1964). A matrix method for elastic wave problems, *Bull. Seism. Soc. Am.* **54**, 431–438.
- Levshin, A. L. (1978). *Surface and Channel Seismic Waves*, Nauka, Moscow, pp. 32–87.
- Mayers, E. P., and A. M. Baptista (1995). Finite element modeling of the July 12, 1993 Hokkaido Nansei-Oki tsunami, *Pure Appl. Geophys.* **144**, 769–803.
- Mooney, W., Laske, G., and T. Masters (1998). Crust 5.1: a global crustal model at  $5^\circ \times 5^\circ$ , *J. Geophys. Res.* **103**, 727–747.
- Novikova, T. (1997). Numerical modeling of the tsunami generation by seismic sources, *Ph.D. Thesis*, Earth Physics Department, Institute of Physics, St. Petersburg University, St. Petersburg, Russia.
- Okal, E. (1978). A physical classification of the Earth's spheroidal modes, *J. Phys. Earth* **26**, 75–103.
- Okal, E. (1988). Seismic parameters controlling far-field tsunami amplitudes: a review, *Natural Hazards* **1**, 67–96.
- Pelayo, A., and D. Wiens (1990). The November 20, 1960 Peru tsunami earthquake: source mechanism of a slow event, *Geophys. Res. Lett.* **17**, 661–664.
- Pod'yapol'sky, G. S. (1968). Excitation of a long gravitational wave in the ocean from a seismic source in the crust, *Izv. AN SSSR, Fizika Zemli* **1**, 7–24, (in Russian).
- Pod'yapol'sky, G. S. (1970). Generation of the tsunami wave by the earthquake, in *Tsunamis in the Pacific Ocean*, W. M. Adams (Editor), East-West Center Press, Honolulu, pp. 19–32.
- Press, F., Harkrider, D., and C. Seafeldt (1961). A fast, convenient program for computations of surface wave dispersion curves in multilayered media, *Bull. Seism. Soc. Am.* **51**, 495–502.
- Randall, M. J. (1967). Fast programs for layered half-space problems, *Bull. Seism. Soc. Am.* **57**, 1299–1315.
- Satake, K. (1985). The mechanism of the 1983 Japan Sea earthquake as inferred from long-period surface waves and tsunamis, *Phys. Earth Planet. Interiors* **37**, 249–260.
- Satake, K. (1995). Linear and nonlinear computations of the 1992 Nicaragua earthquake tsunami, *Pure Appl. Geophys.* **144**, 455–471.
- Schwab, F. (1970). Surface-wave dispersion computations: Knopoff's method, *Bull. Seism. Soc. Am.* **60**, 1491–1520.
- Seno, S. (2000). The 21 September, 1999 Chi-Chi earthquake in Taiwan: implications for tsunami earthquakes, *TAO* **11**, N3, 701–708.
- Shearer, P. (1999). *Introduction to Seismology*, Cambridge University Press, New York.
- Shuto, N. (1991). Numerical simulation of tsunamis: Its present and near future, *Natural Hazards* **4**, 171–191.
- Thomson, W. T. (1950). Transmission of elastic waves through a stratified solid medium, *J. Appl. Phys.* **21**, p. 89.
- Udias, A. (1999). *Principles of Seismology*, Cambridge University Press, New York.
- Utsu, T. (1980). Spatial and temporal distribution of low-frequency earthquakes in Japan, *J. Phys. Earth* **28**, 361–384.
- Ward, S. (1980). Relationships of tsunami generation and an earthquake source, *J. Phys. Earth*, **28**, 441–474.
- Ward, S. (1981). On tsunami nucleation: a point source, *J. Geophys. Res.* **86**, 7895–7900.
- Ward, S. (1982a). On tsunami nucleation: an instantaneous modulated line source, *Phys. Earth Planet. Interiors* **27**, 273–285.
- Ward, S. (1982b). Earthquake mechanisms and tsunami generation: the Kurile Islands event of 13 October 1963, *Bull. Seism. Soc. Am.* **72**, 759–777.
- Watson, T. H. (1970). A note on fast computation of Rayleigh wave dispersion in the multilayered elastic half-space, *Bull. Seism. Soc. Am.* **60**, 161–166.
- Westbrook, G., et al. (1973). Lasser Antilles subduction zone in the vicinity of Barbados, *Nature Phys. Sci.* **244**, 118–120.
- Yamashita, T., and R. Sato (1974). Generation of tsunami by a fault model, *J. Phys. Earth* **22**, 415–440.
- Yamashita, T., and R. Sato (1976). Correlation of tsunamis and sub-oceanic Rayleigh wave amplitudes. Possibility of the use of Rayleigh waves in a tsunami warning system, *J. Phys. Earth* **24**, 397–416.
- Yoshii, Y., et al. (1970). Crustal structure of the Tosa deep-sea terrace and Nankani trough (in Japan), in *Island Arc and Ocean*, M. Hoshino and H. Aoki (Editors), Tokai University Press, Tokyo, 93–103.

Institute of Earth Sciences  
Academia Sinica  
Taipei, Taiwan  
(T.N., B.-S.H.)

Institute of Geophysics  
NCU, Taiwan  
(K.-L.W.)